

Reduced model unifying frequency combs in ring and Fabry-Perot quantum cascade lasers

Carlo Silvestri*, Massimo Brambilla[†], Paolo Bardella[‡], Lorenzo Luigi Columbo[‡]

*School of Electrical Engineering and Computer Science, The University of Queensland, Brisbane, Australia

[†]Dipartimento Interateneo di Fisica, Politecnico e Università degli Studi di Bari, CNR-IFN, Bari, Italy

[‡]Dipartimento di Elettronica e Telecomunicazioni, Politecnico di Torino, Torino, Italy

Abstract—We present a new theoretical model to study the spontaneous formation of frequency combs in quantum cascade lasers (QCLs). This model can reproduce comb emission in both ring and Fabry-Perot (FP) cavities. It consists of a single complex Ginzburg-Landau equation modified by a non-local integral term that accounts for the coupling between forward and backward fields in the FP configuration. The ring case is retrieved by setting this integral term to zero. Numerical simulations based on this model allow for reproducing numerous experimental features, such as the coexistence of amplitude and frequency modulations, linear chirp, and self-starting harmonic combs.

Index Terms—Optical frequency combs, Quantum Cascade Laser, Fabry-Perot, Ring cavity

I. INTRODUCTION

The discovery of the spontaneous formation of optical frequency combs (OFCs) in quantum cascade lasers (QCLs) [1] has sparked a decade of intensive research, focusing on experimental characterization, theoretical investigation of their physical origins, and applications such as spectroscopy and optical communications [2]. From a theoretical perspective, models with reduced mathematical complexity have been crucial in providing insight into the physical mechanisms responsible for the formation of these OFCs [3], [4]. However, there are still unresolved issues in the literature that require further theoretical and modeling efforts, such as the origin of harmonic frequency combs (HFCs), the presence of linear chirp in mid-infrared (mid-IR) QCLs but not in terahertz (THz) devices, and certain differences between ring and Fabry-Perot (FP) combs [5]. We address some of these issues by introducing a reduced model based on a modified complex Ginzburg-Landau equation (CGLE) [6]. This model captures the dynamics of both ring and FP configurations, allowing for a comparative analysis between them. It is equivalent to two coupled CGLEs in the FP case, and to a single conventional CGLE in the ring case, in agreement with previous studies [7]–[9].

II. THEORETICAL MODEL

Starting from the ESMBEs for FP QCLs [10], under the hypotheses of near-threshold operation and fast carriers, we

derive a reduced model consisting of two coupled CGLEs [6]:

$$\begin{aligned} \frac{\partial F^+}{\partial \eta} + \frac{\partial F^+}{\partial t'} &= \sigma \left[(\mu - 1 + i\alpha\mu) F^+ \right. \\ &\quad - 2(1 + i\alpha) (|F^+|^2 + 2K|F^-|^2) F^+ \\ &\quad \left. + \left(\frac{1}{\Gamma^2(1 + i\alpha)} \right) \frac{\partial^2 F^+}{\partial \eta^2} \right] \end{aligned} \quad (1)$$

$$\begin{aligned} -\frac{\partial F^-}{\partial \eta} + \frac{\partial F^-}{\partial t'} &= \sigma \left[(\mu - 1 + i\alpha\mu) F^- \right. \\ &\quad - 2(1 + i\alpha) (|F^-|^2 + 2K|F^+|^2) F^- \\ &\quad \left. + \left(\frac{1}{\Gamma^2(1 + i\alpha)} \right) \frac{\partial^2 F^-}{\partial \eta^2} \right]. \end{aligned} \quad (2)$$

where F^+ and F^- are the counterpropagating field envelopes inside the resonator, σ is the ratio between polarization dephasing time and photon lifetime, μ is the normalized pump rate, α is the LEF, Γ is the normalized gain bandwidth, and η and t' are the scaled spatial and temporal coordinates, respectively. The coefficient K formally parametrizes the coupling between F^+ and F^- due to SHB. $K = 1$ corresponds to the FP case. The unidirectional ring case is retrieved by setting $F^- = 0$ in Eqs. (1)-(2), leading to a single CGLE [7]–[9]. We show that Eqs. (1)-(2) are equivalent to a single modified CGLE with periodic boundary conditions for the auxiliary field $\psi = \sum_{n=-\infty}^{+\infty} f_n e^{i\alpha_n(\eta+t')}$, where f_n are the modal amplitudes of F^+ and F^- , and $\alpha_n = n\pi/L$ [11]:

$$\begin{aligned} \frac{\partial \psi}{\partial t'} &= \sigma \left[(\mu - 1 + i\alpha\mu) \psi - 2(1 + i\alpha) |\psi|^2 \psi \right. \\ &\quad \left. - 4K(1 + i\alpha) \psi \frac{1}{2L'} \int_{-L'}^{L'} d\eta |\psi|^2 + \left(\frac{1}{\Gamma^2(1 + i\alpha)} \right) \frac{\partial^2 \psi}{\partial \eta^2} \right]. \end{aligned} \quad (3)$$

The non local integral term in Eq. (3), proportional to K , accounts for the coupling between the counterpropagating fields due to the SHB. The unidirectional ring case (single conventional CGLE) is obtained by imposing $K=0$. We note that while the equivalence between Eq. (3) and Eqs. (1)-(2) holds only for facet reflectivity $R = 1$, Eqs. (1)-(2), as well as the single CGLE for the ring, can be integrated for any value of R . We remark that the full model ESMBEs and the reduced model are in good qualitative agreement [6].

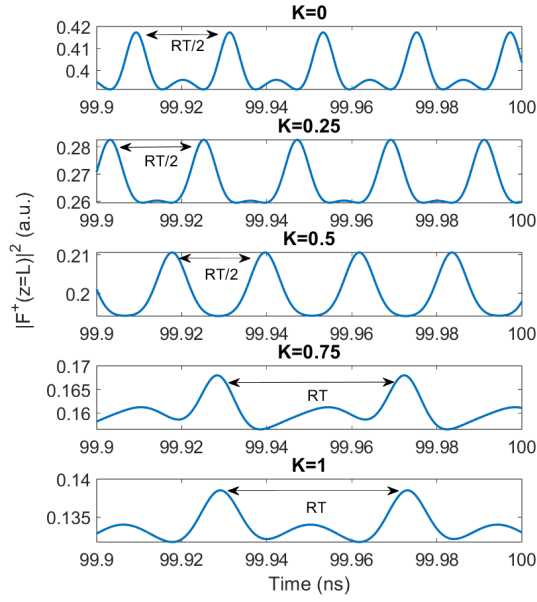


Fig. 1. Temporal evolution of the normalized power for simulated regimes obtained by solving Eq. (3) for different values of the coupling coefficient K .

III. NUMERICAL RESULTS

We investigate the role of the non local integral term in Eq. (3) on the comb formation, by sweeping the coupling coefficient K between 0 (ring) and 1 (FP). The other parameters are $\alpha = 1.15$, $\Gamma = 0.06$, and a cavity length $L = 2$ mm. The temporal evolution of the reconstructed intensity is shown for for the different K values in Fig. 1. We remark that the model is effective in reproducing the OFC regimes in general (for further details, see [6]). We observe the formation of a second order HFC for K between 0 and 0.5, and a transition to a fundamental OFC for $K = 0.75$. For $K=1$ (FP cavity) we also report a fundamental OFC. These results indicate that the integral term is detrimental to the formation of harmonic states, suggesting that HFC formation is favored in the ring configuration compared to the FP. This is confirmed by extensive numerical simulations performed for different (α, Γ) pairs, so that $\alpha \in [1.1, 1.3]$ and $\Gamma \in [0.03, 0.15]$, by integrating the two coupled CGLEs Eqs. (1)-(2) with QCL reflectivity $R = 0.3$. For each pair, the normalized pump parameter $p = \mu/\mu_{\text{thr}}$ is swept between 1 and 2. The other parameters are $\sigma = 4.5 \times 10^{-4}$, kept constant for both configurations, $L = 2$ mm for the FP case and $L = 4$ mm for the ring resonator to ensure the same free spectral range. The parameter values used are typical for THz QCLs. The results are presented in Fig. 2. We observe that harmonic states occur more frequently in the ring cavity than in the FP. Moreover, the simulated ring QCL can generate comb regimes with higher harmonic orders. Specifically, a fourth-order HFC is observed in the ring configuration, while the highest harmonic order reported in the FP configuration is 2. This study underscores the suitability of the presented model for a comparative analysis of the two cavity configurations.

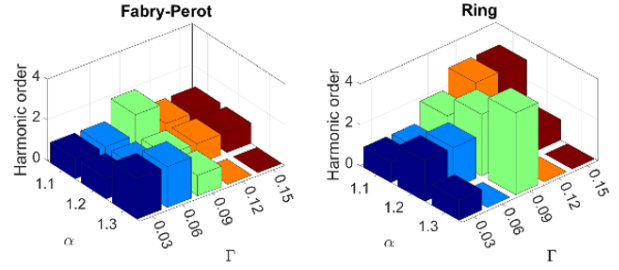


Fig. 2. Maximum harmonic order of the combs reported for various (α, Γ) pairs in both FP and ring configurations.

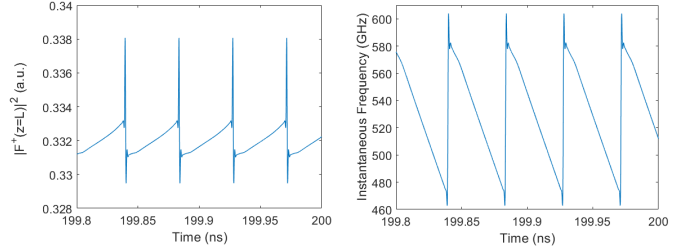


Fig. 3. Normalized power (left) and instantaneous frequency (right) for a dynamical regime obtained with $\Gamma = 1$, resembling typical traces of mid-IR QCL combs [2], [5].

Finally, we report that adopting $\Gamma = 1$, corresponding to a gain curve width of 3.2 THz, we observe temporal traces consistent with those experimentally reported for mid-IR QCLs [2], [5]. These traces exhibit spikes in the power trace and linear chirp in the instantaneous frequency, as shown in Fig. 3. This suggests that a broader gain bandwidth, characteristic of mid-IR QCLs, plays a key role in observing linear chirp, a feature not reported in THz QCLs which are known for narrower gain curves [5].

IV. CONCLUSION

We have introduced a unified reduced model that describes the frequency comb dynamics of both ring and FP QCLs using a single spatiotemporal equation. This model successfully replicates typical experimental features of frequency combs, and its reduced mathematical complexity makes it suitable for underlying physical mechanisms behind these observed phenomena, and for running systematic simulations.

REFERENCES

- [1] Hugi, A. et al., *Nature* 492, 229–233 (2012).
- [2] Piccardo, M. et al., *Laser & Photonics Reviews* 16, 2100403 (2022).
- [3] Opaćak N. et al., *Physical Review Letters* 123, 243902 (2019).
- [4] Burghoff, D. et al., *Optica* 7, 1781-1787 (2020).
- [5] Silvestri, C. et al., *APL Photonics* 8 (2) 020902 (2023).
- [6] Silvestri, C. et al., *arXiv:2403.06486* (2024).
- [7] Piccardo, M. et al., *Nature* 582, 360–364 (2020).
- [8] Colombo, L. L. et al., *Physical Review Letters*, 126, 173903 (2021).
- [9] Opaćak N. et al., *Nature* 625, 685–690 (2024).
- [10] Silvestri, C. et al., *Optics Express*, 28, 23846-23861 (2020).
- [11] Cole, D. C. et al., *Physical Review A*, 98, 013831 (2018).